VIROLOGICA SINICA 2016, 31 (3): 240–248
DOI: 10.1007/s12250-016-3710-z

RESEARCH ARTICLE

Characterization of the viral fibroblast growth factor homolog of *Helicoverpa armigera* single nucleopolyhedrovirus

Feifei Yin[1,2#], Ruikun Du[1#], Wenhua Kuang[1], Guang Yang[1], Hualin Wang[1], Fei Deng[1], Zhihong Hu[1], Manli Wang[1]✉

1. State Key Laboratory of Virology and China Center for Virus Culture Collection, Wuhan Institute of Virology, Chinese Academy of Sciences, Wuhan 430071, China
2. School of Tropical and Laboratory Medicine, Hainan Medical University, Haikou 571101, China

Fibroblast growth factor (FGF) is found throughout multicellular organisms; however, *fgf* homologs (*vfgf*) have only been identified among viruses in lepidopteran baculoviruses. The function of vFGFs from Group I alphabaculoviruses, including *Autographa californica* multiple nucleopolyhedrovirus (AcMNPV) and *Bombyx mori* nucleopolyhedrovirus (BmNPV), involves accelerated killing of infected larvae by both viruses. The vFGF of Group II alphabaculovirus is structurally different from that of Group I alphabaculovirus, with a larger C-terminal region and additional N-linked glycosylation sites. In this study, we characterized the Group II alphabaculovirus vFGF of *Helicoverpa armigera* single nucleopolyhedrovirus (HearNPV). The transcription and expression of *vfgf* was detected at 3 h and 16 h post-infection in HearNPV-infected cells. To further study vFGF function, we constructed *vfgf*-knockout and -repaired HearNPV bacmids and investigated their affect in both cultured cells and insects. Deletion of *vfgf* had no effect on budded-virus production or viral DNA replication in cultured HzAM1 cells. However, bioassays showed that HearNPV *vfgf* deletion significantly increased the median lethal dose and delayed the median lethal time by ~12 h in the host insect when the virus was delivered orally. These results suggested that vFGF is an important virulent factor for HearNPV infection and propagation *in vivo*.

KEYWORDS deletion; function; *Helicoverpa armigera* single nucleopolyhedrovirus (HearNPV); infectivity; *vfgf*

INTRODUCTION

Baculoviridae is a family of rod-shaped, invertebrate-specific DNA viruses with double-stranded, covalently closed, circular genomes ranging from 80–180 kb in size (Lange and Jehle, 2003). Based on molecular phylogenetic analysis, the family is divided into four genera: lepidopteran-specific nucleopolyhedroviruses (NPVs) and granuloviruses are classified as an *Alphabaculovirus* and a *Betabaculovirus*, respectively, and NPVs that infect hymenopteran and dipteran insects are classified as a *Gammabaculovirus* and a *Deltabaculovirus*, respectively (Jehle et al., 2006). The alphabaculoviruses are further divided into Group I and Group II based on phylogenetic analyses (Hayakawa et al., 2000; Herniou et al., 2001; Herniou et al., 2003). Most baculoviruses undergo a biphasic life cycle that generates two virion phenotypes: the occlusion-derived virus (ODV) transmits infection from insect to insect (oral infection), while the budded virus (BV) mediates systemic infection within the infected insect (Funk et al., 1997). Upon ingestion via contaminated food, the occlusion bodies (OBs) dissolve in the alkaline environment of the larval midgut

Received: 27 December 2015, Accepted: 7 April 2016,
Published online: 28 April 2016
# These authors contributed equally to this work.
✉Correspondence:
Phone: +86-27-87197340, Fax: +86-27-87197340
Email: wangml@wh.iov.cn
ORCID: 0000-0001-8701-3530

and release the ODVs, which infect midgut epithelial cells by membrane fusion (Federici, 1997). The tracheae serves as a conduit for progeny virions to cross the basal lamina (BL) into the hemocoel of the insect and establish systemic infection within the insect body (Engelhard et al., 1994).

Fibroblast growth factors (FGFs) are members of a large family of growth factors that are widespread in vertebrates and invertebrates. In vertebrates, 22 members have been identified in the FGF family, sharing highly conserved gene structure and amino acid sequence (Itoh and Ornitz, 2004). FGFs have an array of diverse functions in both developing and adult tissues, including regulating cell proliferation, migration, and differentiation, as well as tissue repair and injury response (Ornitz and Itoh, 2001; Sato and Kornberg, 2002). Although widespread in multicellular organisms, *fgf* homologs have only been identified among viruses in baculoviruses (Detvisitsakun et al., 2007). The lepidopteran baculovirus viral fibroblast growth factors (vFGFs) facilitate dissemination of the virus from infected midgut epithelial cells (Detvisitsakun et al., 2007).

The function of vFGF in Group I alphabaculovirus, including *Autographa californica* multiple nucleopolyhedrovirus (AcMNPV) and *Bombyx mori* nucleopolyhedrovirus (BmNPV), has been studied. Baculovirus vFGFs share a number of properties common to multicellular-organism FGFs, including structural features, extracellular secretion, heparin affinity, and stimulation of insect-cell motility (Katsuma et al., 2004; Detvisitsakun et al., 2005). Deletion of *vfgf* in AcMNPV exhibited no obvious effects on infectious BV production in cultured cells (Detvisitsakun et al., 2006); however, *vfgf* deletion delayed the time of death in *Spodoptera frugiperda* and *Trichoplusiani* larvae when the virus was tested by feeding, but not by intrahemocoelic injection (Detvisitsakun et al., 2007). In contrast to AcMNPV, the BmNPV *vfgf*-knockout mutant produced fewer BVs in cultured cells, but it also took longer to kill the *B. mori* larvae as compared to the wild-type virus when delivered either by feeding or by intrahemocoelic injection (Katsuma et al., 2006b). The roles of vFGF in systemic infection establishment involve remodeling of the BL, which is a tightly woven, virus-impenetrable lining located between the midgut epithelial cells and tracheal cells, and stimulation of tracheoblast migration toward vFGF-expressing cells (Means and Passarelli, 2010). The tracheal system then mediates viral escape from the midgut, carrying the virus to hemocoelic cells and disseminating the infection to other tissues of the infected insects.

Given the functional discrepancies between the two reported vFGFs, it is of interest to investigate the functions of *vfgf* from different baculoviruses. The vFGF of Group II alphabaculoviruses is different from that of Group I alphabaculoviruses, with a larger C-terminal region and more N-linked glycosylation consensus sequences (0–4 for Group I; 3–12 for Group II) that may contribute to vFGF secretion (Katsuma et al., 2004; Katsuma et al., 2006a). In this study, we investigated the function of vFGF from the Group II alphabaculovirus *Helicoverpa armigera* single nucleopolyhedrovirus (HearNPV). In order to elucidate vFGF roles during HearNPV infection *in vitro* and *in vivo*, we characterized *vfgf* transcription and expression profiles and constructed *vfgf*-knockout and -repair HearNPV recombinants. The results suggested that HearNPV *vfgf* play roles in the mortality of host as that of Group I alphabaculoviruses.

MATERIALS AND METHODS

Virus, cell line, and insects

HzAM1 cells were maintained in Grace's insect medium (Gibco-BRL; Life Technologies, Carlsbad, CA , USA) supplemented with 10% fetal bovine serum (Life Technologies) at 28 °C. vHaBac-*egfp-ph* was used as the wild-type control virus (Song et al., 2008) and bHaBacHZ8, an infectious HearNPV bacmid, was used as the parental bacmid (Wang et al., 2003). *H. armigera* larvae were reared on an artificial diet at 27 °C.

Antibody, transcription, and expression analysis

To generate anti-vFGF antibodies, a truncated *vfgf* fragment (70–906 nt) was amplified with the primers anti-vFGF-f and anti-vFGF-r (Supplementary Table S1) using bHaBacHZ8 DNA as the template. The fragment was then cloned into a pET-28a expression vector (Novagen; Merck Millipore, Billerica, MA, USA) and expressed as a His-tag fusion protein in *Escherichia coli* BL21 cells. The fusion protein was purified and used to generate rabbit polyclonal antiserum (anti-vFGF) according to a previously reported method (Wang et al., 2008).

To analyze the transcription and expression profile of HearNPV *vfgf*, 5×10^5 HzAM1 cells were infected with vHaBac-*egfp-ph* at a multiplicity of infection (MOI) of 10 50% tissue-culture infection dose units/cell. At 0, 3, 6, 12, 24, 36, 48, and 72 h post-infection (h.p.i.), cells were collected and washed with phosphate-buffered saline (Figure 1B and 1C). For transcriptional analysis, total DNA-free RNA harvested from the infected cells at each time point was isolated by Trizol reagent (Invitrogen, Carlsbad, CA, USA), and the first-strand cDNA was synthesized with oligo (dT) primers (Promega, Madison, WI, USA) using M-MLV reverse transcriptase (Promega, Madison, WI, USA). The cDNA was then amplified with primers vFGF-trans-f and vFGF-trans-r (Supplementary Table S1). After DNase I treatment, RNA

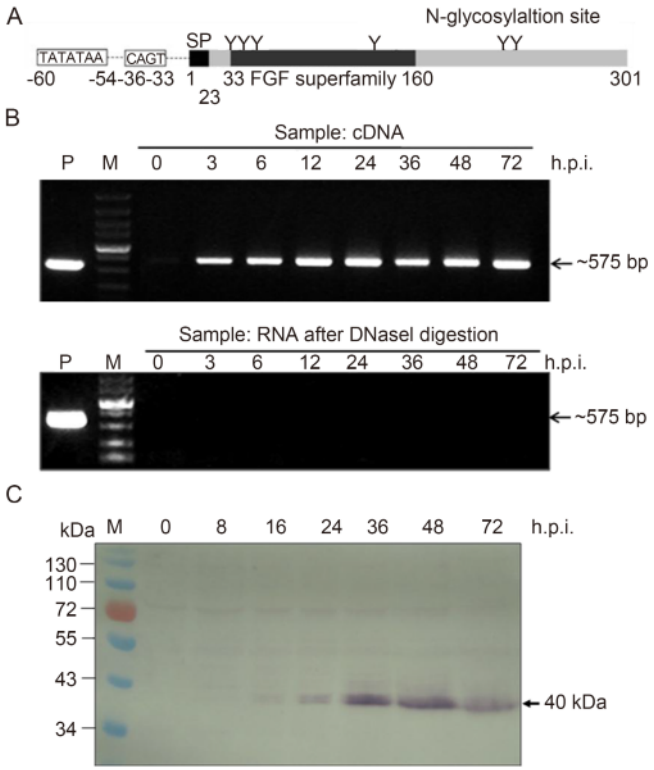

Figure 1. Transcription and expression analyses of vFGF. (A) Schematic representation of HearNPV vFGF. The relative positions of the predicted signal peptide (SP), N-glycosylation sites, and early promoter are shown. (B) Time-course analysis of vFGF transcription. HzAM1 cells were infected with HearNPV BV at an MOI of 10 and collected at the indicated post-infection time points. Total cellular RNA after DNaseI treatment was determined by RT-PCR (upper panel). RNA in each sample after treatment with DNaseI was assessed for DNA contamination by PCR (lower panel). Total DNA in infected cells collected at 72 h.p.i. was used as a positive control. (C) Time-course analysis of vFGF expression. HzAM1 cells were infected with vHaBac-*egfp-ph* at an MOI of 10 and collected at the indicated post-infection time points. Cellular proteins were separated by 10% SDS-PAGE, and the western blot was probed with anti-vFGF polyclonal antibody. The *vfgf* bands are indicated by arrows. M, DNA or protein molecular marker.

from each sample was also tested by PCR for DNA contamination.

For expression analysis, protein samples were separated by sodium dodecyl sulfate polyacrylamide gel electrophoresis (SDS-PAGE; 10% acrylamide gel) and electroblotted onto a nitrocellulose membrane. The blot was probed with anti-vFGF as the first antibody and goat anti-rabbit IgG conjugated with alkaline phosphatase as the secondary antibody (Jackson ImmunoResearch, West Grove, PA, USA). The final signals were detected with 5-Bromo-4-chloro-3-indolyl phosphate and nitro blue tetrazolium.

Construction of the *vfgf*-null HearNPV bacmid

The *vfgf* gene from bHaBacHZ8 was knocked out using a modified form of a previously reported method (Hou et al., 2002). The flanking sequences of the *vfgf* gene were PCR amplified using bHaBacHZ8 as a template and the primers del-F1f/del-F2r and del-F2f/del-F2r (Supplementary Table S1). PCR products were confirmed by sequencing and cloned into the pKS-egfp-cat plasmid (kindly provided by Prof. J.M. Vlak, Wageningen University), which contains the enhanced green fluorescent protein (*egfp*) gene under control of the HSP70 promoter and the chloramphenicol resistance gene (*cat*) (Luo et al., 2011). The resulting plasmid was designated pKS-F_1-*egfp-cat*-F_2. The fragment containing the *egfp* and *cat* genes flanked by F_1 and F_2 was then excised from pKS-F_1-*egfp-cat*-F_2 using *Kpn* I and *Xba* I restriction enzymes to obtain a 3.3-kb fragment, which was gel purified and transformed into *E. coli* BW25113 electrocompetent cells containing bHaBacHZ8 and the helper plasmid pKD46 to generate bHaBac-Δ*vfgf-egfp* (Figure 2A) (Hou et al., 2002). Positive clones resistant to both kanamycin and chloramphenicol were confirmed by PCR.

Construction of the *vfgf*-repaired bacmid

To construct the *vfgf*-repaired bacmid, the *vfgf* gene under its native promoter was PCR amplified with the primers vfgf-f and vfgf-r (Supplementary Table S1) from bHaBacHZ8 using Pyrobest DNA Polymerase (TaKaRa, Kusatsu, Japan). The PCR product was cloned into the pGEM-T Easy vector (Promega) and subjected to sequence confirmation. The *vfgf* fragment was digested from the vector and cloned into the transfer vector pFB-DUAL-*ph* (Song et al., 2008) to generate pFB-DUAL-*vfgf-ph*. The expression cassette was transposed into bHaBac-Δ*vfgf-egfp* by Tn7-mediated transposition according to the Bac-to-Bac Baculovirus Expression Systems manual (Invitrogen), and the resulting bacmid was designated as bHaBac-REP*vfgf-egfp-ph* (Figure 2A). The polyhedrin (*ph*) gene was reintroduced into bHaBac-Δ*vfgf-egfp* to produce bHaBac-Δ*vfgf-egfp-ph* using the previously constructed pFB-DUAL-*ph*, since the original *ph* was disrupted during the construction of bHaBacHZ8 (Figure 2A). The previously constructed bHaBac-*egfp-ph* containing the *egfp-cat* cassette and *ph* was used as a positive control (Song et al., 2008).

Transfection and infection assay

HzAM1 cells (5.0×10^5/well) were transfected with 2 μg DNA of each recombinant bacmid using 12 μL of Lipo-

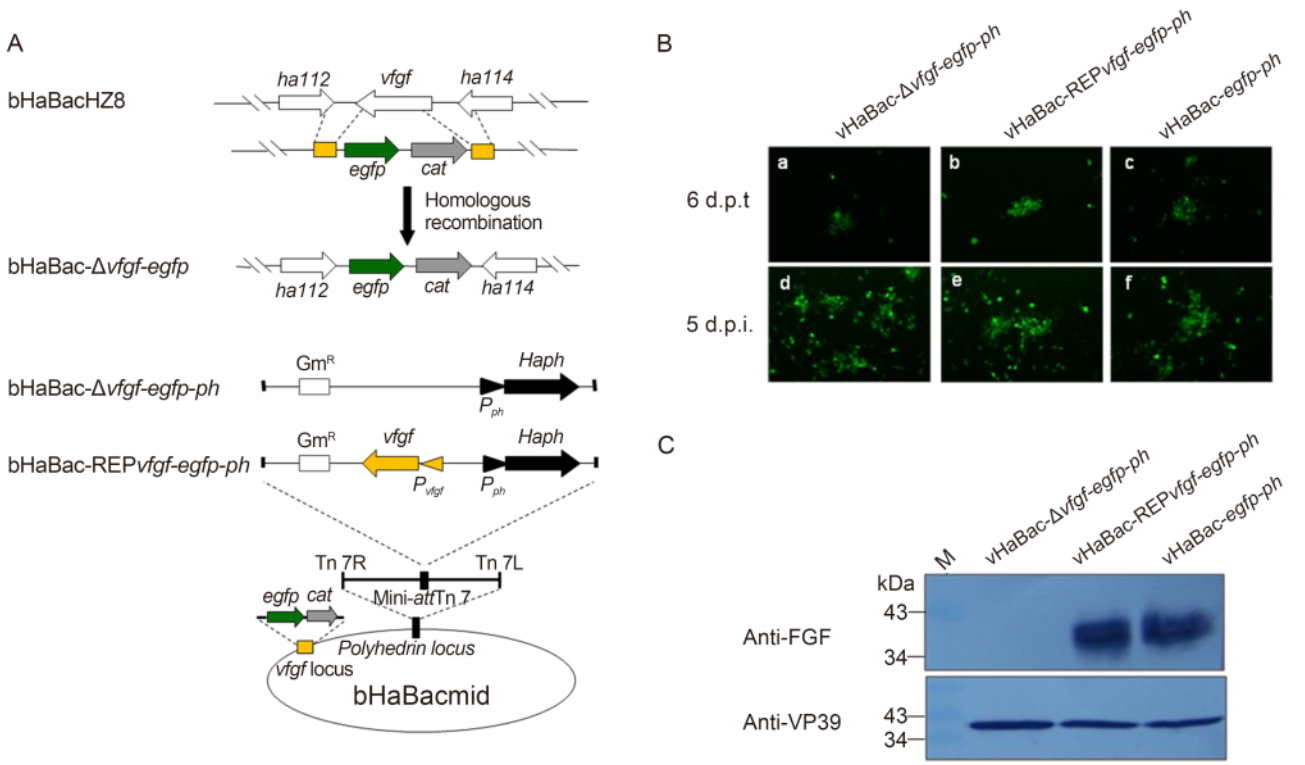

Figure 2. Construction and verification of recombinant HearNPVs. (A) Construction of the recombinant HearNPV bacmids. The fragment containing the *egfp* and *cat* genes flanked by *vfgf* homologous arms was used for homologous recombination to generate bHaBac-Δ*vfgf-egfp*. The *ph* gene was reintroduced into bHaBac-Δ*vfgf-egfp* by Tn7-mediated transposition to produce bHaBac-Δ*vfgf-egfp-ph*. The *ph* gene together with *vfgf* under the control of its own promoter were inserted at the *ph* locus of bHaBac-Δ*vfgf-egfp* to generate bHaBac-REP*vfgf-egfp-ph*. Previously constructed bHaBac-*egfp-ph* containing the *egfp-cat* cassette and *ph* gene was used as a positive control. (B) Transfection-infection assays of recombinant bacmids. Each recombinant bacmid DNA was transfected into HzAM1 cells (a, b, and c). At 6 d.p.t., clarified supernatant was used to infect healthy HzAM1 cells (d, e and f). The transfected and infected cells were monitored by fluorescence microscopy. (C) Western blot detection of recombinant viruses. BVs of each recombinant virus were collected from the supernatant of infected cells, purified by ultracentrifugation, and electrophoresed by 10% SDS-PAGE. The expression of vFGF was detected with anti-vFGF antibody, and the major capsid protein VP39 was used as an internal control. M, protein molecular marker; d.p.i., days post-infection.

fectin reagent (Invitrogen) according to the Bac-to-Bac Baculovirus Expression Systems manual. At 6 days post-transfection (d.p.t.), cell supernatants were harvested by centrifugation at 945×*g* for 5 min and then used to infect another batch of HzAM1 cells. Green cells were monitored by fluorescence microscopy daily for the successful transfection and spread of infection. For BV amplification, HzAM1 cells were infected at an MOI of 0.1, and the supernatant was collected at 6 days post-infection.

One-step growth-curve analysis

For the virus growth curves, 3×10^5 HzAM1 cells were infected with vHaBac-Δ*vfgf-egfp-ph*, vHaBac-REP*vfgf-egfp-ph*, or vHaBac-*egfp-ph* at an MOI of 10. Supernatants were harvested at 0, 12, 24, 48, 72, and 96 h.p.i., and BV titers were determined by end-point dilution assays (EPDAs). Infection experiments were performed in triplicate, and the mean BV titers were analyzed using one-way analysis of variance (SPSS Inc., Chicago, IL, USA) with virus type and time as factors (Yin et al., 2008).

Viral DNA-replication assay

To detect viral DNA replication in infected cells, HzAM1 cells (3×10^5) were infected with vHaBac-Δ*vfgf-egfp-ph* or vHaBac-*egfp-ph* at an MOI of 10. Total cellular DNA was isolated at 0, 24, and 48 h.p.i. using Genomic DNA Rapid Isolation Kit (BioDev, Beijing, China). Primers *Ha39*-F and *Ha39*-R designed previously were used to determine viral copy numbers in total cellular DNA according to previously reported methods (Huang et al., 2014).

Bioassays

To investigate the effect of *vfgf* deletion on HearNPV infectivity, bioassays were performed as described previously (Sun et al., 2009; Luo et al., 2011). The median lethal dose (LD_{50}) of ODV was determined with third-instar *H. armigera* larvae using the food-contamination method with eight different doses of occlusion bodies (OBs): 1×10^3, 3×10^3, 1×10^4, 3×10^4, 1×10^5, 3×10^5, 1×10^6, and 3×10^6. After inoculation, the larvae were transferred to a fresh diet and maintained separately at 27 °C in 24-well plates. Twenty-four insects were inoculated for each dose, and mortality was checked daily. Each test was performed twice. The data from two replicates were pooled to calculate the final LD_{50} values when there was no significant difference between replicate results. LD_{50} values and the confidence limits of different variants were determined by probit analysis (SPSS Inc.) and compared by standard lethal-dose ratio comparison (Robertson et al., 2007).

The median survival time (ST_{50}) of third-instar *H. armigera* larvae dosed with different variants was determined using a food-contamination method as described previously (Luo et al., 2011). Briefly, 1×10^6 OBs were applied to a small piece of artificial diet and after completely ingesting the contaminated food, the larvae were further reared using an uncontaminated diet. Forty-eight insects were tested for each virus, and mortality was checked every 6 h. ST_{50} values were calculated using a Kaplan-Meier estimator and compared using the log-rank test.

RESULTS

Transcription and expression analysis of HearNPV vFGF

The *fgf* gene of HearNPV encodes a ~40-kDa protein containing 302 amino acids and six predicted N-linked glycans (Figure 1A). An early-transcription-initiation motif, TATATAA, followed by CAGT (18 nt downstream from TATA), was found 54 nt upstream of the ATG translation start codon of *vfgf* (Figure 1A), suggesting that *vfgf* is an early gene. In fact, we detected *vfgf* transcripts (575 bp) by reverse transcription (RT)-PCR analysis at 3 h.p.i. (Figure 1B), and western blot analysis indicated a protein band with the expected size of vFGF (~40 kDa) at 16 h.p.i. (Figure 1C). Given that HearNPV genomic DNA replication begins at ~14 h.p.i. (Dai et al., 2006), *vfgf* was suggested to be an early gene of HearNPV, with its expression continuing into the later stages of infection.

Construction and verification of *vfgf*-deleted and -repaired HearNPVs

To determine *vfgf* function in HearNPV infectivity, the *vfgf* gene from bHaBacHZ8 was inactivated by homologous recombination and replaced by an *egfp-cat* cassette, with the resulting bacmid designated as bHaBac-Δ*vfgf-egfp* (Figure 2A). Two recombinant bacmids were constructed based on bHaBac-Δ*vfgf-egfp*: a *vfgf*-knockout bacmid (bHaBac-Δ*vfgf-egfp-ph*), where the *ph* gene was re-inserted into the *ph* locus; and a *vfgf*-repaired bacmid (bHaBac-REP*vfgf-egfp-ph*), where the *ph* gene and *vfgf* under the control of its own promoter were inserted into the *ph* locus (Figure 2A). A previously constructed bacmid (bHaBac-*egfp-ph*) containing *egfp* and *ph* was used as a positive control (Luo et al., 2011). Using a transfection-infection assay, the effect of *vfgf* deletion on BV propagation was monitored by fluorescence microscopy (Figure 2B). Infection was observed in cells incubated with bHaBac-Δ*vfgf-egfp-ph*-transfected cell supernatant, indicating that *vfgf* is nonessential for *in vitro* viral replication and infection (Figure 2B-a and B-d). Transfection-infection of the *vfgf*-repaired bacmid and the positive-control bacmid revealed results similar to those observed with bHaBac-REP*vfgf-egfp-ph* (Figure 2B-b, c, e and f).

The absence of vFGF in HaBac-Δ*vfgf-egfp-ph* BVs was confirmed by western blot analysis. With anti-vFGF antiserum, no specific band was detected in BV samples harvested from the supernatant of vHaBac-Δ*vfgf-egfp-ph*-infected HzAM1 cells. In contrast, a band of ~40 kDa was clearly detected in BV samples from vHaBac-REP*vfgf-egfp-ph*- and vHaBac-*egfp-ph*-infected cells (Figure 2C). The expression of VP39 indicated that similar BV concentrations were loaded into each lane (Figure 2C). These results confirmed the correct construction of all of the recombinants.

The effect of *vfgf* deletion on infectious BV production and viral DNA replication *in vitro*

To study the effect of *vfgf* on infectious BV production, one-step growth curves were determined and compared. HzAM1 cells were infected with vHaBac-Δ*vfgf-egfp-ph*, vHaBac-REP*vfgf-egfp-ph*, or vHaBac-*egfp-ph* in parallel (MOI=10). Supernatants collected at different post-infection time points were titrated by EPDA. The results showed that vHaBac-Δ*vfgf-egfp-ph*, vHaBac-REP*vfgf-egfp-ph*, and vHaBac-*egfp-ph* exhibited similar kinetics of infectious BV production (Figure 3A). Statistical analysis also revealed that there was no significant difference between *vfgf*-knockout and -repaired viruses or with the control virus at all infection time points ($P > 0.05$).

To further illustrate the effect of *vfgf* deletion on viral DNA synthesis, the level of viral DNA replication during infection was monitored by real-time PCR analysis. The results indicated that there was no significant difference in viral DNA copy number between vHaBac-Δ*vfgf-egfp-ph*- and vHaBac-*egfp-ph*-infected cells at both 24

and 48 h.p.i. ($P > 0.05$; Figure 3B). These results indicated that *vfgf* deletion had no significant influence on either infectious BV production or viral DNA replication in cultured cells.

The contribution of vFGF to viral infectivity in infected insects

To determine the LD_{50} value of vHaBac-Δ*vfgf-egfp-ph*, vHaBac-REP*vfgf-egfp-ph*, and vHaBac-*egfp-ph*, third-instar *H. armigera* larvae were infected orally with various doses of OBs and monitored for mortality. The LD_{50} value of vHaBac-Δ*vfgf-egfp-ph* was 16.9 (12.4, 22.7) $\times 10^3$ OBs, which was significantly higher than that of vHaBac-REP*vfgf-egfp-ph* or vHaBac-*egfp-ph* ($P < 0.05$), while no significant difference was observed between the LD_{50} values of vHaBac-REP*vfgf-egfp-ph* or vHaBac-*egfp-ph* ($P > 0.05$) (Table 1). We also compared the time required to kill infected larvae, with the results indicating that the ST_{50} value of vHaBac-Δ*vfgf-egfp-ph* (~107 h) was significantly higher than that of vHaBac-*egfp-ph* (~95 h; $P < 0.05$), while no significant difference was observed between the ST_{50} values of vHaBac-REP*vfgf-egfp-ph* or vHaBac-*egfp-ph* ($P > 0.05$). These data indicated that *vfgf* deletion resulted in a delayed time of death of larvae infected orally (Table 2). Taken together, these results suggested that *vfgf* deletion significantly reduced HearNPV infectivity in larvae.

DISCUSSION

The *vfgf* gene is conserved in most lepidopteran baculoviruses sequenced to date. The function of the *vfgf* of Group I alphabaculovirus has been studied and was suggested to play a role in dissemination of viral infection from the midgut of the insect host (Detvisitsakun et al., 2006; Katsuma et al., 2006b; Detvisitsakun et al., 2007). The function of vFGF was also suggested to be dependent upon activation of matrix metalloproteases and effector caspases, leading to BL alteration and stimulation of tracheoblast and midgut epithelial cell migration (Means and Passarelli, 2010). Compared to Group I alphabaculovirus vFGF, the vFGF of Group II alphabaculoviruses has a larger C-terminal region and more putative N-glycosylation sequences. Here, we investigated the function of HearNPV vFGF, with results indicating that *vfgf* deletion had no clear impact on BV production or viral DNA replication in cultured cells. In the host insects, the lack of *vfgf* resulted in reduced infectivity and a delayed time of death of larvae when delivered by feeding.

The transcription and expression pattern of HearNPV *vfgf* was investigated at various time points following

Table 1. Dose-mortality responses of vHaBac-*egfp-ph*, vHaBac-Δ*vfgf-egfp-ph*, and vHaBac-REP*vfgf-egfp-ph* in third-instar *H. armigera* larvae

Viruses	$LD_{50} \times 10^3$ OBs (95% CI)	Potency ratio[a] (95% CI)
vHaBac-*egfp-ph*	9.2 (6.7, 12.5)	–
vHaBac-Δ*vfgf-egfp-ph*	16.9 (12.4, 22.7)	1.8* (1.2, 2.9)
vHaBac-REP*vfgf-egfp-ph*	8.7 (6.4, 12.0)	0.9 (0.6, 1.5)

Note: [a] Potency ratio was calculated by dividing the LD_{50} of the *vfgf*-deleted or -repaired variants by that of vHaBac-*egfp-ph*. * Indicates significant difference based on the 95% CI of the potency ratio, including the value 1.0 (Robertson et al., 2007). CI, confidence interval.

Table 2. Time-mortality responses of vHaBac-*egfp-ph*, vHaBac-Δ*vfgf-egfp-ph*, and vHaBac-REP*vfgf-egfp-ph* in third-instar *H. armigera* larvae.

Tests	Viruses	ST_{50} (95% CI) (h)	χ^2	*P*
1	vHaBac-*egfp-ph*	95 (93.2, 96.7)	–	–
	vHaBac-Δ*vfgf-egfp-ph*	107.5 (103.1, 111.9)	27.834	1×10^{-6} *
	vHaBac-REP*vfgf-egfp-ph*	94.5 (93.1, 95.9)	3.568	0.059
2	vHaBac-*egfp-ph*	95 (93.1, 96.9)	–	–
	vHaBac-Δ*vfgf-egfp-ph*	107.5 (104.5, 110.5)	19.915	8×10^{-6}*
	vHaBac-REP*vfgf-egfp-ph*	94.5 (93.6, 95.4)	3.327	0.068

Note: * Indicates significant difference between the *vfgf*-deleted variant and vHaBac-*egfp-ph* based on log-rank test. CI, confidence interval.

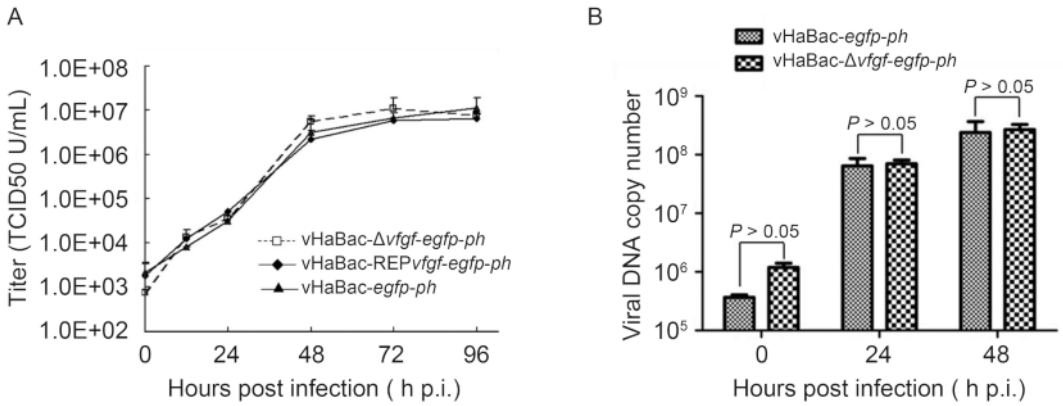

Figure 3. Effect of vFGF on viral growth kinetics and DNA replication. (A) One-step growth-curve analysis of BV production. HzAM1 cells were infected with either vHaBac-Δ*vfgf-egfp-ph*, vHaBac-REP*vfgf-egfp-ph*, or vHaBac-*egfp-ph* at an MOI of 10. BVs were harvested at the indicated post-infection time points and titrated onto HzAM1 cells. Each data point represents the average titer from three independent infections, and error bars represent standard deviations. (B) Real-time PCR analysis of viral DNA replication. HzAM1 cells were infected with the respective virus at an MOI of 10. At the indicated post-infection time points, total cellular DNA was isolated, digested with *Dpn* I, and subjected to real-time PCR analysis. The experiments were performed in triplicate, and error bars represent standard deviations. TCID50, 50% tissue-culture infection dose.

HearNPV infection. The transcription of *vfgf* was detected as early as 3 h.p.i., suggesting that *vfgf* is an HearNPV early gene (Figure 1B), and a baculovirus consensus early promoter was also found in the upstream region of the *vfgf*-translation start codon. Additionally, BmNPV *vfgf* was identified as an early gene, although no typical baculovirus promoter motifs were found (Katsuma et al., 2004). For some viruses, such as *Epiphyas postvittana* MNPV and *Chrysodeixis chalcites* NPV, no consensus baculovirus *vfgf*-promoter motifs were detected (Hyink et al., 2002; Oers et al., 2005), while baculovirus late-promoter motifs were found associated with the *vfgf* from *Ectropis obliqua* nucleopolyhedrovirus, *Mamestra configurata* NPV, and *Lymantria dispar* multinucleocapsid NPV (Kuzio et al., 1999; Li et al., 2002; Ma et al., 2007). This suggested that *vfgf* transcriptional regulation may vary among baculoviruses, and that the transcription pattern may not be strictly related to *vfgf* phylogeny.

Genomic sequence comparison revealed that most alphabaculoviruses encode one *vfgf* homolog, even though there are three *vfgf* homologs (vFGF-1, 2, and 3) identified in betabaculovirus. (Yin et al., 2015). Sequence analysis revealed that HearNPV vFGF contains a typical FGF-superfamily central motif of ~120 amino acids essential for binding to an FGF receptor, which is also present in Group I alphabaculovirus vFGFs (Figure 1A) (Popovici et al., 2005). In contrast, the FGF-superfamily central motif of betabaculovirus vFGFs is much shorter (~30 amino acids) and nontypical (data not shown). Therefore, HearNPV vFGF appears to share greater similarity with Group I alphabaculovirus vFGFs relative to those from betabaculoviruses based on conservation of a structural domain and potential function. Functional analysis indicated that *vfgf* deletion did not influence ODV morphogenesis or occlusion (data not shown), but significantly impaired HearNPV infectivity in larvae (Table 1 and 2). We speculated that HearNPV vFGF may also play a role in dissemination of virus infection from the midgut as proposed in previous studies of Group I vFGFs; however, confirmation requires further evidence.

Although AcMNPV and BmNPV are closely related Group I alphabaculoviruses, the function of their vFGFs differ significantly. A study of AcMNPV revealed that a *vfgf* knockout exhibited no significant *in vitro* effect on DNA and protein syntheses or BV production (Detvisitsakun et al., 2007). In contrast, *vfgf* deletion in BmNPV reduced BV production in both cultured cells and infected larvae (Katsuma et al., 2006b). Furthermore, the expression of late and very late genes was also reduced in *vfgf*-deficient BmNPV (Katsuma et al., 2006b). In our study, we observed that HearNPV *vfgf* deletion did not influence either BV production (Figure 3A) or the expression of late and very late viral genes (data not shown), implying that the *in vitro* function of HearNPV vFGF is much closer to that reported for AcMNPV as compared to BmNPV. In larval bioassays, both the LD_{50} and ST_{50} values of *vfgf*-deleted HearNPV increased; however, only the latter increased in *vfgf*-deleted AcMNPV or BmNPV. The different phenotypes associated with vFGF-deleted baculoviruses may be determined by the coaction of different vFGFs and host species. We are currently constructing recombinant HearNPVs wherein

the *vfgf* gene is replaced with counterparts from other viruses in order to more effectively compare the functions of vFGFs in the same viral backbone and host systems.

In summary, this is the first report concerning the function of vFGF from a Group II alphabaculovirus. Our results indicated that HearNPV vFGF transcription begins at the early stage of infection and continues into the late stage of infection. These *in vitro* experiments showed that the lack of *vfgf* did not influence HearNPV viral growth kinetics or DNA replication, while *vfgf* deletion significantly impaired HearNPV infectivity in larvae. Therefore, vFGF represents an important virulent factor associated with *in vivo* HearNPV infection.

ACKNOWLEDGMENTS

This work was supported by grants from the National Science Foundation of China (No. 31200124 and 31321001) and the Strategic Priority Research Program of the Chinese Academy of Sciences (Grant No. XDB11030400). We acknowledge the Core Facility and Technical Support of Wuhan Institute of Virology for technical assistance. The authors would like to thank Dr. Xiulian Sun for the great help in statistical analysis.

COMPLIANCE WITH ETHICS GUIDELINES

The authors declare that they have no conflicts of interest. This article does not contain any studies with human or animal subjects performed by any of the authors.

AUTHOR CONTRIBUTIONS

FFY, ZHH, HLW, and MLW designed the experiments. FFY, RKD, WHK, and GY performed the experiments. FFY, FD, and HLW analyzed the data. FFY, ZHH, and MLW wrote the paper. All the authors approved the final manuscript.

Supplementary Table are available on the website of *Virologica Sinica*: www.virosin.org; link.springer.com/journal/12250.

REFERENCES

Dai W, Deng F, Wang H, Yuan L, Hu Z. 2006. The Transcription Profiles of Nine HaSNPV Genes. Virol Sin, 21: 47–51.

Detvisitsakun C, Berretta MF, Lehiy C, Passarelli AL. 2005. Stimulation of cell motility by a viral fibroblast growth factor homolog: proposal for a role in viral pathogenesis. Virology, 336: 308–317.

Detvisitsakun C, Cain EL, Passarelli AL. 2007. The Autographa californica M nucleopolyhedrovirus fibroblast growth factor accelerates host mortality. Virology, 365: 70–78.

Detvisitsakun C, Hutfless EL, Berretta MF, Passarelli AL. 2006. Analysis of a baculovirus lacking a functional viral fibroblast growth factor homolog. Virology, 346: 258–265.

Engelhard EK, Kam-Morgan LNW, Washburn J, Volkman LE. 1994. The insect tracheal system: A conduit for the systemic spread of Autographa californica M nuclear polyhedrosis virus. Proc Natl Acad Sci USA, 91: 3224–3227.

Federici BA. 1997. Baculovirus pathogenesis. In: *The baculoviruses*, Miller LK (ed. New York, N.Y: Plenum Press, pp. 33–60.

Funk CJ, Braunagel SC, Rohrmann GF. 1997. Baculovirus structure. In: *The baculoviruses*, Miller LK (ed). New York: Plenum Press, pp. 7–32.

Hayakawa T, Rohrmann GF, Hashimoto Y. 2000. Patterns of genome organization and content in lepidopteran baculoviruses. Virology, 278: 1–12.

Herniou EA, Luque T, Chen X, Vlak JM, Winstanley D, Cory JS, O'Reilly DR. 2001. Use of whole genome sequence data to infer baculovirus phylogeny. J Virol, 75: 8117–8126.

Herniou EA, Olszewski JA, Cory JS, O'Reilly DR. 2003. The genome sequence and evolution of baculoviruses. Annu Rev Entomol, 48: 211–234.

Hou S, Chen X, Wang H, Tao M, Hu Z. 2002. Efficient method to generate homologous recombinant baculovirus genomes in E. coli. BioTechniques, 32: 783–789.

Huang H, Wang M, Deng F, Hou D, Arif BM, Wang H, Hua Z. 2014. The ha72 Core Gene of Baculovirus Is Essential for Budded Virus Production and Occlusion-Derived Virus Embedding, and Amino Acid K22 Plays an Important Role in Its Function. J Virol, 88: 705–709.

Hyink O, Dellow RA, Olsen MJ, Caradoc-Davies KMB, Drake K, Herniou EA, Cory JS, O'Reilly DR, Ward VK. 2002. Whole genome analysis of the Epiphyas postvittana nucleopolyhedrovirus. J Gen Virol, 83: 957–971.

Itoh N, Ornitz DM. 2004. Evolution of the Fgf and Fgfr gene families. Trends Genet, 20: 563–569.

Jehle JA, Blissard GW, Bonning BC, Cory JS, Herniou EA, Rohrmann GF, Theilmann DA, Thiem SM, Vlak JM. 2006. On the classification and nomenclature of baculoviruses: a proposal for revision. Arch Virol, 151 1257–1266.

Katsuma S, Daimon T, Horie S, Kobayashi M, Shimada T. 2006a. N-linked glycans of Bombyx mori nucleopolyhedrovirus fibroblast growth factor are crucial for its secretion. Biochem Biophys Res Commun, 350: 1069–1075.

Katsuma S, Horie S, Daimon T, Iwanaga M, Shimada T. 2006b. *In vivo* and *in vitro* analyses of a Bombyx mori nucleopolyhedrovirus mutant lacking functional vfgf. Virology, 355: 62–70.

Katsuma S, Shimada T, Kobayashi M. 2004. Characterization of the baculovirus Bombyx mori nucleopolyhedrovirus gene homologous to mammalian FGF gene family. Virus Genes, 29: 211–217.

Kuzio J, Pearson MN, Harwood SH, Funk CJ, Evans JT, Slavicek JM, Rohrmann GF. 1999. Sequence and Analysis of the Genome of a Baculovirus Pathogenic for Lymantria dispar. Virology, 253: 17–34.

Lange M, Jehle JA. 2003. The genome of the Cryptophlebia leucotreta granulovirus. Virology, 317: 220–236.

Li Q, Donly C, Li L, Willis LG, Theilmann DA, Erlandson M. 2002. Sequence and Organization of the Mamestra configurata Nucleopolyhedrovirus Genome. Virology, 294: 106–121.

Luo S, Zhang Y, Xu X, Westenberg M, Vlak JM, Wang H, Hu Z, Deng F. 2011. Helicoverpa armigera nucleopolyhedrovirus occlusion-derived virus-associated protein, HA100, affects oral infectivity in vivo but not virus replication in vitro. J Gen Virol, 92: 1324–1331.

Ma X, Shang J, Yang Z, Bao Y, Xiao Q, Zhang C. 2007. Genome sequence and organization of a nucleopolyhedrovirus that infects the tea looper caterpillar, Ectropis obliqua. Virology, 30: 235–246.

Means JC, Passarelli AL. 2010. Viral fibroblast growth factor, matrix metalloproteases, and caspases are associated with enhancing systemic infection by baculoviruses. Proc Natl Acad Sci U S A, 107: 9825–9830.

Oers MMv, Abma-Henkens MHC, Herniou EA, Groot JCWd, Peters S, Vlak aJM. 2005. Genome sequence of Chrysodeixis chalcites nucleopolyhedrovirus, a baculovirus with two DNA photolyase genes. J Gen Virol, 86: 2069–2080.

Ornitz DM, Itoh N. 2001. Fibroblast growth factors. Genome Biol, 2: 3005.3001–3005.3012

Popovici C, Roubin R, Coulier F, Birnbaum D. 2005. An evolutionary history of the FGF superfamily. Bioessays, 27: 849–857.

Robertson JL, Savin NE, Preisler HK, Russell RM. 2007. Bioassays with Arthropods CRC Press, Boca Raton. page?

Sato M, Kornberg TB. 2002. FGF is an essential mitogen and chemoattractant for the air sacs of the Drosophila tracheal system. Dev Cell, 3: 195–207.

Song J, Wang R, Deng F, Wang H, Hu Z. 2008. Functional studies of per os infectivity factors of Helicoverpa armigera single nucleocapsid nucleopolyhedrovirus. J Gen Virol, 89: 2331–2338.

Sun X, Wu D, Sun X, Jin L, Ma Y, Bonning BC, Peng H, Hu Z. 2009. Impact of Helicoverpa armigera nucleopolyhedroviruses expressing a cathepsin L-like protease on target and nontarget insect species on cotton. Biol Control, 49: 77–83.

Wang H, Deng F, Pijlman GP, Chen X, Sun X, Vlak JM, Hu Z. 2003. Cloning of biologically active genomes from a Helicoverpa armigera single-nucleocapsid nucleopolyhedrovirus isolate by using a bacterial artificial chromosome. Virus Res, 97: 57–63.

Wang M, Tan Y, Yin F, Deng F, Vlak JM, Hu Z, Wang H. 2008. The F protein of *Helicoverpa armigera* single nucleopolyhedrovirus can be substituted functionally with its homologue from Spodoptera exigua multiple nucleopolyhedrovirus. J Gen Virol, 89: 791–798.

Yin F, Wang M, Tan Y, Deng F, Vlak JM, Hu Z, Wang H. 2008. A functional F analogue of Autographa californica nucleopolyhedrovirus GP64 from the Agrotis segetum granulovirus. J Virol, 82: 8922–8926.

Yin F, Zhu Z, Liu X, Hou D, Wang J, Zhang L, Wang M, Kou Z, Wang H, Deng F, Hu Z. 2015. The Complete Genome of a New Betabaculovirus from Clostera anastomosis. PLoS One, 10: e0132792.